Measurement of the Casimir force in a gas and in a liquid

Anne Le Cunuder,[1,*] Artyom Petrosyan,[1] George Palasantzas,[2] Vitaly Svetovoy,[2,3] and Sergio Ciliberto[1]

[1]*Laboratoire de Physique, CNRS UMR5672, Université de Lyon, École Normale Supérieure, 46 Allée d'Italie, 69364 Lyon, France*
[2]*Faculty of Sciences and Engineering, University of Groningen, Nijenborg 4, 9747 AG Groningen, The Netherlands*
[3]*A. N. Frumkin Institute of Physical Chemistry and Electrochemistry, Russian Academy of Sciences,
Leninsky prospect 31 bld. 4, 119071 Moscow, Russia*

We present detailed measurements of the Casimir-Lifshitz force between two gold surfaces, performed in both gas (nitrogen) and liquid (ethanol) environments with the same apparatus and on the same spot of the sample. Furthermore, we study the role of double-layer forces in the liquid, and we show that these electrostatic effects are important. The latter contributions are subtracted to recover the genuine Casimir force, and the experimental results are compared with calculations using Lifshitz theory. Our measurements demonstrate that carefully accounting for the actual optical properties of the surfaces is necessary for an accurate comparison with the Lifshitz theory predictions at distances smaller than 200 nm.

Introduction. As devices enter the submicron range, Casimir forces [1–12] between neutral bodies at close proximity become increasingly important. As Casimir first understood in 1948 [2], these forces are due to the confinement of quantum fluctuations of the electromagnetic (EM) field. Indeed, Casimir proved that when two parallel, perfectly reflecting plates, are introduced in vacuum, they impose, on the EM field, boundary conditions which select only the fluctuations compatible with them. As a result, an attractive force between the plates is produced, which depends only on fundamental constants, on the distance d between the surfaces, and on their area A:

$$F_c(d) = -\frac{\pi^2 A \hbar c}{240 d^4} \quad (1)$$

with $\hbar$ the Planck constant and c the speed of light. Following Casimir's calculation [2], Lifshitz and co-workers in the 1950s [3] considered the more general case of real dielectric plates by exploiting the fluctuation-dissipation theorem, which relates the dissipative properties of the plates and EM fluctuations at equilibrium. Furthermore, for real surfaces, roughness and material optical properties can strongly alter the Casimir force [13,14].

Lifshitz formalism describes the Casimir force in a general case, where the medium between the plates need not be vacuum. According to this formalism, the force can be tuned from attractive to repulsive with a suitable choice of the interacting materials. These predictions boosted Casimir experiments to test the possibility of repulsive forces [15]. In liquids, the determination of the Casimir force is more complex than in a gas because of the presence of additionnal effects, as, e.g., the Debye screening. The Casimir-Lifshitz force has been measured between two gold surfaces immersed in ethanol [16]; in

this experiment, electrostatic forces are found to be negligible as sodium iodide (NaI) was added to ethanol, decreasing the Debye screening length. However, the role of electrostatic forces and their screening by the Debye layer are important and one has to consider carefully their contributions during force measurements in liquids [17,18]. In order to clarify the interplay of the Casimir force and additional effects in liquids, we have performed measurements of the Casimir force in a nitrogen atmosphere in the first place, and then, using the same system and sample, in ethanol. The contact area is the same in both measurements. We observe that electrostatic forces, screened over the Debye length, are of the same magnitude as the Casimir force, in the 50–200 nm distance range. After subtracting the electrostatic force, we obtain a Casimir force in quantitative agreement with Lifshitz theory [3]. Furthermore, the accuracy of our measurement allows us to highlight the importance of accurately characterizing the optical properties of the samples before any meaningful comparison with theory.

Experimental setup. We use an atomic force microscope to measure the Casimir force between metallic surfaces. In order to measure the force with a good accuracy, the cantilever displacement is measured with a homemade quadrature phase interferometer [19], whose operating principle is sketched in Fig. 1.

The experiment is performed in a sphere-plane geometry to avoid the need to maintain two flat plates perfectly parallel. Thus, a polystyrene sphere of radius $R = (75.00 \pm 0.25)$ μm (Sigma-Aldrich) is mounted on the tip of the cantilever with a conductive glue and then the whole probe is coated by a gold film whose thickness is about 100 nm. The plates have been gold coated using cathodic sputtering by ACM [20], at the LMA-CNRS [21]. The diameter of the sphere has been determined from scanning electron microscopy. We use a cantilever (size 500 μm × 30 μm × 2.7 μm, NanoAndMore) of stiffness $\kappa = 0.57 \pm 0.03$ N/m. The precise value of κ is determined using equipartition, i.e., $\langle \delta^2 \rangle = \frac{k_B T}{\kappa}$, where k_B is

---
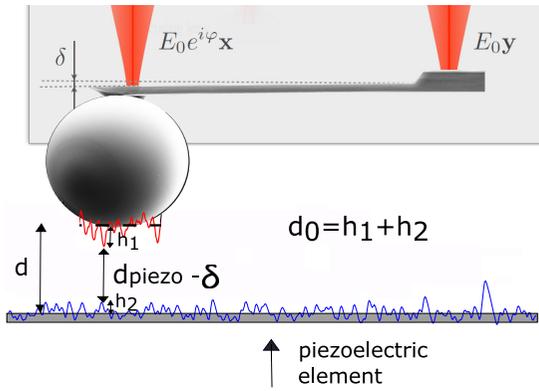
FIG. 1. Experimental setup. A gold-coated polystyrene bead is glued on the cantilever tip which measures the sphere-plane interaction force at distance d. The deflection of the cantilever is detected by an interferometric technique: two laser beams, orthogonally polarized, are focused on the cantilever; the reference one is reflected by the static base and the second one by the cantilever free end. When the cantilever is bent the optical path difference δ between the two beams is measured through an interferometer [19].

the Boltzmann constant and T the temperature. The resonance frequency of the sphere-cantilever ensemble is $f_o = 2271$ Hz in vacuum.

The sphere faces a glass flat plate which is coated by a gold film of a thickness of about 100 nm [22]. According to [23], the layer is sufficiently thick to be considered as a bulklike film. The plate is mounted on a piezoactuator (PZ38; Piezojena) which allows us to control the plane-sphere distance. During the experiment, the plate is moved continuously toward the sphere and the induced deflexion of the cantilever is detected by the interferometer.

In air, because of water vapor, the capillary force far exceeds the Casimir force. Therefore, our measurement in a gas was performed after filling our cell with nitrogen.

Calibrations. The total force between the surfaces is the sum of the Casimir force $F_{Cas}(d)$ and additional contributions:

$$F_{total} = F_{Czzas}(d) + F_{el}(d) + F_H(d, v). \quad (2)$$

Electrostatic forces $F_{el}(d)$ are due to a potential difference between surfaces, owing to differences between the work functions of the materials used, and the possible presence of trapped charges [24]. Hydrodynamic forces $F_H(d, v)$ are due to the motion of the fluid during the approach of the plate toward the sphere, and depend on their relative velocity v [25]. These hydrodynamic effects are negligible in a nitrogen atmosphere, where the viscosity is $\gamma = 1.76 \times 10^{-6}$ Pas, but have to be considered in ethanol where the viscosity is 1000 times higher ($\gamma = 1.2 \times 10^{-3}$ Pas).

There are two main requirements for a precise determination of the Casimir force. Firstly, additional forces must be measured with accuracy and subtracted from the total measured force. Secondly, because the force has a strong dependence on the distance between surfaces, an independent measure of the distance is necessary, which becomes difficult when the separation approaches nanometer scales. The difficulty originates principally from surface roughness: when the two surfaces come into contact, the highest asperities of each

surface touch each other and the surfaces are still separated by a distance upon contact d_0 [26].

The piezoactuator includes a position sensor which gives us the displacement of the plate: d_{piezo}. We define the origin of d_{piezo} as the position of contact of the highest peak of the sphere roughness with the surface of the plate, as the sphere is much rougher than the plate. The effective separation distance which appears in the expression of the force can be written as (see Fig. 1)

$$d = d_{piezo} + d_0 - \delta, \quad (3)$$

where d_0 is the distance upon contact due to surface roughness and δ is an additional correction which results from the static deflection of the cantilever in response to the total force F_{total}.

We determined the separation upon contact d_0 from hydrodynamic calibration, performed in ethanol. Immediatly after measuring the Casimir force in nitrogen, we carefully injected ethanol into the cell, and we performed calibrations and measurements of the Casimir force in ethanol. As the horizontal drift of our system is negligible, the contact area and the separation distance upon contact d_0 are the same in each measurement. This assumption is further justified *a posteriori*: our experimental curves all superimpose on top of each other and on top of the theoretical curve after shifting the distance by the same value of d_0. The hydrodynamic calibration is presented in the next section, while topographic analysis is presented in [22]. The value of d_0 obtained from hydrodynamic calibration is comparable with the value obtained from roughness analysis.

Hydrodynamic calibration in ethanol. The theoretical expression of the hydrodynamic force, for nonslip boundary conditions, is given by [25]

$$F_H = -\frac{6\pi \eta R^2}{d} v, \quad (4)$$

where η is the fluid viscosity, R is the radius of the sphere, and $v = \frac{\partial d}{\partial t}$ is the relative velocity between the plate and the sphere. Indeed, in our case, the slippage can be neglected as the mean free path is in the order of intermolecular distances (e.g., a few angstroms), and negligible in comparison with the roughness of the surface (e.g., a few tens of nanometers) [27].

As is clear from Eq. (2), among the different forces occurring between the surfaces, the hydrodynamic force is the only one which depends on velocity. Thus we performed two force measurements, continuously moving the plate toward the sphere: a first one at velocity $v_1 = 348$ nms^{-1}, and a second one at a velocity $v_2 = 5109$ nms^{-1}. By taking the difference between these two measurements, we canceled all the velocity-independent forces and from Eq. (4) we obtained F_H measured at $v = v_2 - v_1 = 4742$ nms^{-1}:

$$F_{total}(d, v_2') - F_{total}(d, v_1') = F_H(d, v). \quad (5)$$

Here, v_2' and v_1' are the relative velocities between the sphere and the sample, which are not exactly the piezovelocities v_2 and v_1 because the cantilever is deflected when the plate is moved toward the sphere. v_2' and v_1' were determined precisely measuring the deflection of the cantilever.

Measurements of the hydrodynamic force are presented in [22]. Comparing the measured hydrodynamic force with the theoretical expression of Eq. (4), we determined the separation distance upon contact $d_0 = (31 \pm 2)$ nm.

Electrostatic forces. Even if the surfaces are as clean as possible, there always remain electrostatic forces between them. First, an electrostatic potential difference V_c still exists between clean, grounded, metallic surfaces owing to differences between the work functions of the materials used [24]. Second, electrostatic forces can remain due to the presence of trapped charges. In liquids, these trapped charges induce double-layer forces, due to the rearrangement of ions in solution, screening the electrostatic interactions.

When $d \ll R$, the expression of the electrostatic force is [28,29]

$$F_e = -\frac{\pi \epsilon_0 \epsilon_d R}{\lambda_D} V_c^2 \exp(-d/\lambda_D). \qquad (6)$$

The term $\frac{V_c^2}{d}$ is the contribution of the contact potential V_c between the surfaces and the term $\exp(-d/\lambda_D)$ represents the double-layer force, screened over a distance λ_D (the Debye length) [30].

As there is no free charge in nitrogen, the Debye length is infinite and the electrostatic interaction is not screened, consequently there are no double-layer forces. In nitrogen, the contact potential was calibrated to $V_c = (87 \pm 2)$ mV, and was compensated by an applied voltage difference during the measurement of the Casimir force.

In contrast, in ethanol, the contact potential is strongly screened by the ions constituting the Debye layer. Moreover, applying an electrostatic potential in a polar liquid can yield a transient current [31] and consequently, charges accumulate on surfaces, preventing us from applying the method suggested in [32] to cancel the Debye force. Therefore, we simply subtracted the contribution of electrostatic forces from force measurements, after determining $\lambda_D = (46 \pm 6)$ nm

and $V_c = (63 \pm 13)$ mV [22]. In ethanol V_c is lowered because the dissociation of molecules at the surface leads to the formation of a first very thin screening layer of a few nanometers.

Measurement of the Casimir force in nitrogen. Static measurements of the Casimir force were carried out in a nitrogen atmosphere, between a gold-coated sphere and a gold-coated plate. We subtracted the vertical thermal drift by fitting linearly each force curve measurement between 300 nm and 1 μm and subtracting it from each measured curve. All force curves were shifted in distance corresponding to the separation upon contact $d_0 = 31$ nm.

The measured Casimir force is shown in Fig. 2(a) for separations ranging from 90 to 370 nm, averaging 28 independent measurements. For theoretical calculations, thermal corrections are negligible as the thermal energy $k_B T$ is too small to populate the mode of lowest energy $\hbar c / \lambda_T$, as the separation distance d satisfies

$$d < 370 \text{ nm} \ll \lambda_T = \frac{\hbar c}{k_B T} \approx 7 \text{ } \mu\text{m}, \quad \text{at } 300 \text{ K}. \qquad (7)$$

We compared our experimental result with theoretical predictions of the Casimir force, based on optical properties of Au taken from (1) the handbook of tabulated data (green dashed-dotted line) [33] and (2) measurements on Au samples presenting the same roughness and preparation conditions as ours (orange solid line) [10].

The deviation from Lifshitz theory based on dielectric properties of real samples is less than 5 pN at closest separations, while it reaches 10 pN at closest separations for calculations based on data from the handbook. As the signal-to-noise ratio degrades with increasing distance, the deviation of the measurements from Lifshitz theory increases at larger distances. However, they remain compatible within the error bars, including systematic and statistical errors (dominant
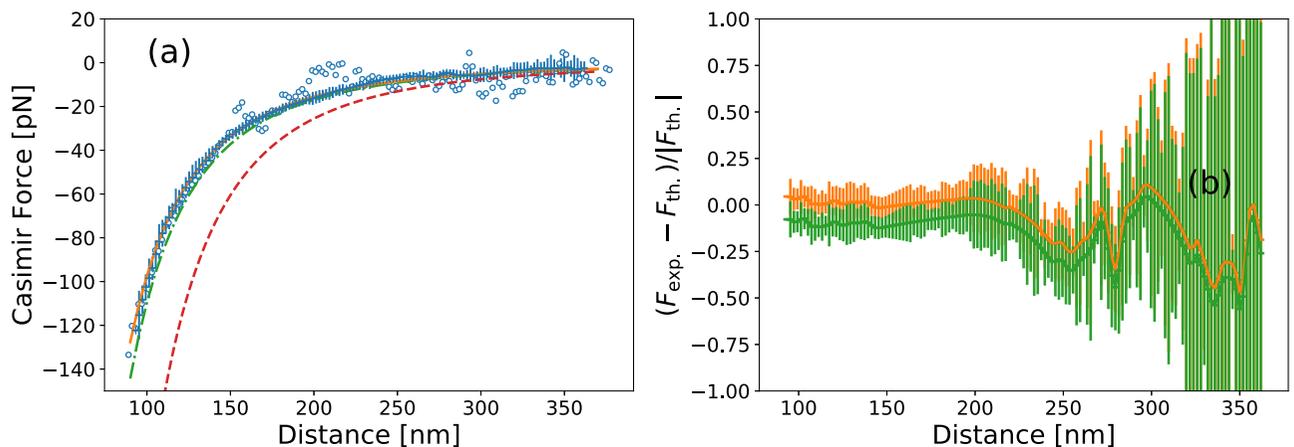
FIG. 2. Measurement of the Casimir force between two Au surfaces in a nitrogen atmosphere. (a) Blue points correspond to the mean measured force. Blue circles correspond to a single measurement of the Casimir force. Orange solid curve corresponds to the Lifshitz theory in which the dielectric function ϵ is evaluated from measured optical data of a real gold film [10]. For the green dashed-dotted line, ϵ is evaluated using the handbook optical data [34]. Red dashed line corresponds to the theory in the case of ideal conductors. (b) Relative difference between the theoretical and experimental Casimir forces. Same colors as in (a). The error bars include the statistical and the systematic errors due to uncertainties on the separation upon contact $d_0 = (31 \pm 2)$ nm (using the hydrodynamic estimation), on the stiffness $\kappa = (0.57 \pm 0.03)$ N/m and on the diameter of the sphere $D = (150.0 \pm 0.5)$ μm.
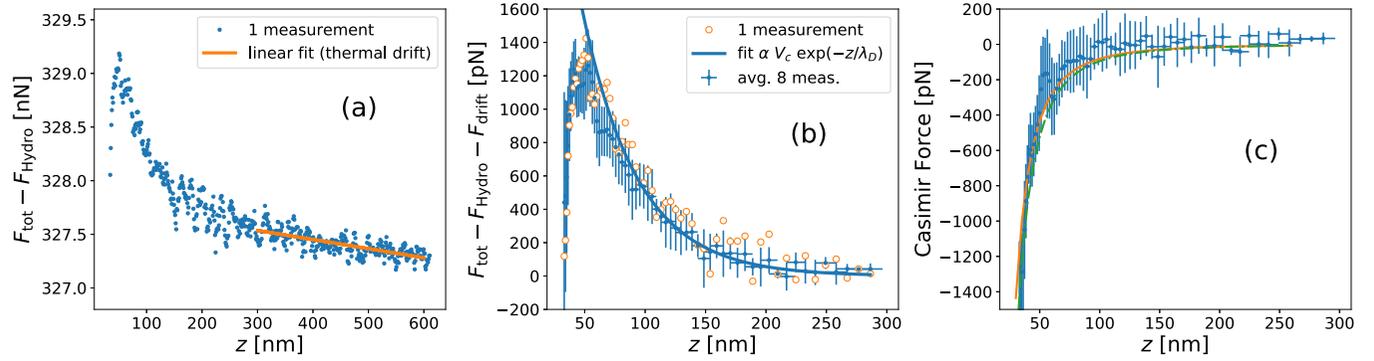
FIG. 3. Measurement of the Casimir force in ethanol. (a) Single force measurement (blue points) after subtracting the hydrodynamic force. The distance has been shifted by $d_0 = 31$ nm. The red line corresponds to the linear fit of the thermal drift in the range 300–600 nm. (b) Single force measurement (red circles) and mean force measurement (blue points) (averaged over eight measurements) of $F_{cas} + F_{Debye}$ obtained after subtraction of the thermal drift and the hydrodynamic force. The mean measured force is fitted by an exponential in the range $d > 120$ nm. In this distance range, double-layer forces largely remove the Casimir force. The blue line corresponds to the exponential fit, yielding the Debye length $\lambda_D = (46 \pm 6)$ nm and the surface potential $\psi_{0_{adj}} = (63 \pm 13)$ mV through Eq. (6). (c) Measurement of the Casimir force between two Au surfaces in ethanol, where blue crosses correspond to the mean measured force. The orange solid line corresponds to the Lifshitz theory where the dielectric function ϵ is evaluated from measured optical data of a real gold film [10]; for the green dashed-dotted line, ϵ is evaluated using the handbook optical data [34].

at large distances). This demonstrates that surfaces must be carefully characterized for high precision measurements of the Casimir force. In order to make this argument more quantitative, we present the difference $(F_{exp} - F_{th})/F_{th}$ in Fig. 2(b), showing the differences between the theoretical and experimental Casimir forces, for calculations based on data from the handbook and calculations based on dielectric properties measured on films with the same morphology as our films.

Measurement of the Casimir force in ethanol. In a liquid, the scenario is richer than in a gas because of the presence of additional effects, namely, the hydrodynamic force and the Debye screening of the electrostatic interactions.

Measurements in ethanol were performed with the same apparatus, immediately after the measurement in nitrogen, so that the contact area would be the same, as explained previously. During the measurement of the Casimir force, the approach velocity was chosen in order to compromise between the hydrodynamic force F_H we wanted to minimize and vertical drift, limiting the time of measurement. The results presented in this Rapid Communication were obtained with 100 nms^{-1}.

In order to average the data collected from consecutive runs, eight data sets were acquired. First, all force curves were shifted in distance corresponding to the separation distance upon contact $d_0 = 31$ nm. Second, the hydrodynamic force F_H was subtracted from each measurement independently. As the F_H dependence on distance is accurately known [22], it can be safely subtracted from the measured force. Third, to remove vertical thermal drift from force measurement, each force curve was fitted linearly between 300 and 600 nm. Figure 3(a) shows a single force measurement in ethanol after subtracting the hydrodynamic force. Blue points correspond to the raw measurement, and the red line corresponds to the linear fit of the thermal drift, which is then subtracted from each measurement. In Fig. 3(b), we represent both a single force measurement (blue) and the average measured

force (red), after subtracting the thermal drift and the hydrodynamic force. The remaining force shows the presence of repulsive forces at separation distances larger than 60 nm. These repulsive forces are attributed to the presence of ions in solution and on metallic surfaces. Then, the remaining curve corresponding to $F_{Cas} + F_{Debye}$ was averaged over eight measurements and the mean curve was fitted by an exponential function $A \exp(-d/\lambda_D)$ in the distance range $d > 120$ nm. A and λ_D are adjustable parameters. In this distance range, we assume that the Casimir force is negligible in comparison to the double-layer force (as predictions of the Lifshitz theory indicate). We obtained a Debye length $\lambda_D = (46 \pm 6)$ nm consistent with measurements reported by [35] and [36]. The exponential fit is also used to determine the electrostatic potential at the gold surface ψ_0 from the expression of the double-layer force in a sphere-plane geometry: $F = 4\pi\epsilon\epsilon_0 R \psi_0^2 / \lambda_D e^{-d/\lambda_D}$. We evaluated the surface potential $\psi_{0_{adj}} = (63 \pm 13)$ mV. After subtracting the measured double-layer force from each force measurement, the measured Casimir force is obtained. The measured Casimir force is presented in Fig. 3(b). The experimental data are compared to Lifshitz's theory for a gold sphere of radius $R = 75$ μm and a gold plate separated from a distance d in ethanol. Finally, the differences between the theoretical predictions and the measured data are plotted in Fig. 3(c). In spite of the rather large error bars we can distinguish the two theoretical predictions: Casimir force measurements are in better agreement with Lifshitz theory based on optical properties of real Au films, presenting the same morphology as ours.

Conclusion. In conclusion, we have presented measurements of the Casimir force performed both in gas (nitrogen) and liquid (ethanol) environments with the same apparatus and on the same spot of the sample. The force measurements yield experimental evidence of the importance of electrostatic effects in ethanol. These effects were properly measured and subtracted, in order to determine the genuine Casimir force. Furthermore, these measurements demonstrate that the

Casimir force is sensitive to changes in the optical properties of gold at distances of less than 200 nm mostly in the gas environment where the force is the strongest. Our measurements are of significant interest given the fundamental implications of the Casimir force in the search of new hypothetical forces, technology applications of Casimir forces for micro/nano device actuation [1,37], and the very timely nature of our measurements [38].

[1] C. Genet, F. Intravaia, A. Lambrecht, and S. Reynaud, *Annales de la Fondation Louis de Broglie* (Conservatoire national des arts et métiers, 2003).

[2] H. B. G. Casimir, Indag. Math. **10**, 261 (1948) [Kon. Ned. Akad. Wetensch. Proc. **100**(3–4), 61 (1997)].

[3] E. M. Lifshitz, Sov. Phys. JETP **2**, 73 (1956).

[4] S. K. Lamoreaux, Phys. Rev. Lett. **78**, 5 (1997).

[5] D. Iannuzzi, M. Lisanti, and F. Capasso, Proc. Natl. Acad. Sci. USA **101**, 4019 (2004).

[6] F. Chen, G. L. Klimchitskaya, V. M. Mostepanenko, and U. Mohideen, Opt. Express **15**, 4823 (2007).

[7] C.-C. Chang, A. A. Banishev, G. L. Klimchitskaya, V. M. Mostepanenko, and U. Mohideen, Phys. Rev. Lett. **107**, 090403 (2011).

[8] S. de Man, K. Heeck, R. J. Wijngaarden, and D. Iannuzzi, Phys. Rev. Lett. **103**, 040402 (2009).

[9] G. Torricelli, P. J. van Zwol, O. Shpak, C. Binns, G. Palasantzas, B. J. Kooi, V. B. Svetovoy, and M. Wuttig, Phys. Rev. A **82**, 010101 (2010).

[10] V. B. Svetovoy, P. J. van Zwol, G. Palasantzas, and J. T. M. De Hosson, Phys. Rev. B **77**, 035439 (2008).

[11] A. A. Banishev, C.-C. Chang, R. Castillo-Garza, G. L. Klimchitskaya, V. M. Mostepanenko, and U. Mohideen, Phys. Rev. B **85**, 045436 (2012).

[12] R. S. Decca, D. López, E. Fischbach, G. L. Klimchitskaya, D. E. Krause, and V. M. Mostepanenko, Phys. Rev. D **75**, 077101 (2007).

[13] V. Svetovoy and G. Palasantzas, Adv. Colloid Interface Sci. **216**, 1 (2015).

[14] W. Broer, G. Palasantzas, J. Knoester, and V. B. Svetovoy, Phys. Rev. B **85**, 155410 (2012).

[15] J. N. Munday, F. Capasso, and V. A. Parsegian, Nature (London) **457**, 170 (2009).

[16] J. N. Munday and F. Capasso, Phys. Rev. A **75**, 060102 (2007).

[17] B. Geyer, G. L. Klimchitskaya, U. Mohideen, and V. M. Mostepanenko, Phys. Rev. A **77**, 036102 (2008).

[18] J. N. Munday and F. Capasso, Phys. Rev. A **77**, 036103 (2008).

[19] L. Bellon, Exploring nano-mechanics through thermal fluctuations, Ph.D. thesis, Ecole Normale Supérieure de Lyon ENS LYON, 2010, 176 pages.

[20] http://www.acm-pvd.com/en/

[21] http://lma.in2p3.fr/

[22] See Supplemental Material at http://link.aps.org/supplemental/10.1103/PhysRevB.98.201408 for a detailed discussion of (1) the roughness analysis of the surfaces; (2) the hydrodynamic calibration of the separation distance upon contact; and (3) the measurement of the contact potential, and which contains the additional references [10,24,26,39,40].

[23] M. Lisanti, D. Iannuzzi, and F. Capasso, Proc. Natl. Acad. Sci. USA **102**, 11989 (2005).

[24] C. C. Speake and C. Trenkel, Phys. Rev. Lett. **90**, 160403 (2003).

[25] H. Brenner, Chem. Eng. Sci. **16**, 242 (1961).

[26] P. J. van Zwol, V. B. Svetovoy, and G. Palasantzas, Phys. Rev. B **80**, 235401 (2009).

[27] R. I. P. Sedmik, A. F. Borghesani, K. Heeck, and D. Iannuzzi, Phys. Fluids **25**, 042103 (2013).

[28] J. Laurent, Casimir force measurements at low temperature, Ph.D. thesis, Université de Grenoble, 2010.

[29] J. Laurent, H. Sellier, A. Mosset, S. Huant, and J. Chevrier, Phys. Rev. B **85**, 035426 (2012).

[30] H. J. Butt and M. Kappl, *Surface and Interfacial Forces* (Wiley-VCH, Weinheim, 2010).

[31] T. Fort and R. L. Wells, Surf. Sci. **12**, 46 (1968).

[32] D. S. Ether, F. S. S. Rosa, D. M. Tibaduiza, L. B. Pires, R. S. Decca, and P. A. Maia Neto, Phys. Rev. E **97**, 022611 (2018).

[33] E. D. Palik, *Handbook of Optical Constants of Solids* (Academic Press, New York, 1997).

[34] E. D. Palik, *Handbook of Optical Constants of Solids* (Academic Press, New York, 1998), Vol. 3.

[35] P. J. van Zwol, G. Palasantzas, and J. T. M. DeHosson, Phys. Rev. E **79**, 041605 (2009).

[36] J. N. Munday, F. Capasso, V. A. Parsegian, and S. M. Bezrukov, Phys. Rev. A **78**, 032109 (2008).

[37] V. B. Svetovoy and M. V. Lokhanin, Mod. Phys. Lett. A **15**, 1013 (2000).

[38] J. L. Garrett, D. A. T. Somers, and J. N. Munday, Phys. Rev. Lett. **120**, 040401 (2018).

[39] M. Sedighi, V. B. Svetovoy, and G. Palasantzas, Phys. Rev. B **93**, 085434 (2016).

[40] S. de Man, K. Heeck, and D. Iannuzzi, Phys. Rev. A **82**, 062512 (2010).